Supporting information material

Experimental section

Materials

All solvents and reagents obtained from commercial suppliers were used without further purification.
Cu(II) and Zn(II) ion sources, respectively the hydrated salts, $CuCl_2 \cdot 2H_2O$ and $ZnSO_4 \cdot 7H_2O$, L(+)-ascorbic acid sodium salt, L-glutathione reduced (GSH), TCEP (tris(2-carboxyethyl)phosphine hydrochloride), HCl (trace metal grade), PAR (4-(2-pyridylazo)resorcinol), EDTA (ethylenediaminetetraacetic acid), Tris base (Trizma, 2-amino-2-(hydroxymethyl)-1,3-propanediol), POBN (α-(4-pyridyl N-oxide)-N-tert-butylnitrone), tetrakis(acetonitrile)copper(I) hexafluorophosphate (Cu(I) source) were purchased from Sigma-Aldrich. The Fe source was an Fe(III) standard solution purchased from Fluka Analytical (1.001 g/l). Trypton, yeast extract, LB Broth, agar, agarose, IPTG (isopropyl-β-D-1 thiogalactopyranoside), SDS (sodium dodecyl sulfate), HEPES (*N*-2-hydroxyethylpiperazine-*N*'-2-ethanesulfonic acid) were from Lab Empire, NaCl, NaOH, glycerol, $KH_2PO_4 \cdot H_2O$, K_2HPO_4 from POCH (Gliwice Poland), pTYB21 vector and chitin resin from New England BioLabs. DTNB (5,5'-dithiobis-(2-nitrobenzoic acid)) from TCI Europe N.V., DTT (DL-dithiothreitol) from Iris Biotech. All solutions were prepared with Milli-Q water obtained with a deionizing water system (Merck).
Ligands: 3-aminopyridine-2-carboxaldehyde thiosemicarbazone (3-AP), di-2-pyridylketone-4,4,-dimethyl-3-thiosemicarbazone (Dp44mT) were purchased from Sigma Aldrich (purity ≥ 98%). Pyridine-2-carboxaldehyde thiosemicarbazone (PT) was purchased from Enamine Store (purity ≥ 95 %).

Methods

Protein expression and purification

Two different batches of Zn_7MT-1 protein from mouse were used. 1) Zn_7MT-1 overexpressed in *Escherichia coli* strain BL21(pLysS) which was purified as previously described.[1] Such batch was used for the experiments monitored by absorbance and EPR spectroscopy. 2) Zn_7MT-1 recombinantly produced in the laboratory of Dr. Ricard Albalat (University of Barcelona) as previously reported.[2] Such batch of protein was used for the MS experiments.
The coding cDNA sequences of human metallothionein-1e (MT-1e), metallothionein-2a (MT-2a) and metallothionein-3 (MT-3) were purchased from GenScript (USA) and cloned into the pTYB21 vector (New England Biolabs). The expression vectors were transformed into BL21(DE3)pLysS *E. coli* component cells and the protein was expressed as intein fusion.[3] The bacteria were cultured (depending on isoform 4-6 × 1 l) in rich full growth medium (1.1% tryptone, 2.2% yeast extract, 0.45% glycerol, 1.3% K_2HPO_4, 0.38% KH_2PO_4) until OD600 reached 0.5 at 37°C, then induced with 0.1 mM IPTG and incubated overnight at 20°C with vigorous shaking.[4] Cells were collected by centrifugation at 4 000 × *g* for 10 min at 4°C, suspended in 200 ml cold buffer A (20 mM HEPES, pH 8.0, 500 mM NaCl, 1 mM EDTA, 1 mM TCEP) and sonicated for 30 min followed by centrifugation at 20,000 × *g* for 45 min at 4°C. Clear supernatants were incubated with 10 ml of a chitin resin (New England Biolabs) overnight with mild shaking at 4°C. The resin was than washed 5-6 times with 25 ml of the same buffer and the cleavage reaction was initiated by adding DTT to a final concentration of 100 mM in buffer A without TCEP. Metallothionien proteins were cleaved from resin for 48 h at room temperature with mild mixing. The eluted supernatants containing MT-1e, MT-2 and MT-3 were acidified to pH ca. 2.5 using 7% HCl and concentrated using Amicon Ultra-4 Centrifugal Filter Units (Millipore). The concentrated apoproteins were purified using a SEC-70 column (Bio-Rad) equilibrated with 10 mM HCl using Bio-Rad

NGC system. The identity of the protein was confirmed using mass spectrometry, on an API 2000 ESI-MS instrument (Applied Biosystems). The averaged molecular masses found/calculated were 6014.4/6014.1, 6043.3/6042.2 and 6925.2/6927.0 for MT-1e, MT-2 and MT-3, respectively. Apoproteins were mixed with 10 molar equivalents of $ZnSO_4$ in the presence of 2 mM TCEP under anaerobic conditions (argon atmosphere).[5] The pH of the solution was adjusted to 8.6 using 1 M Tris base. The sample was concentrated similarly as above and purified on SEC-70 column equilibrated with 20 mM Tris-HCl, pH 8.6. The collected fractions with MT proteins were concentrated and used immediately for experiments or stored at -80°C. The concentrations of Zn(II) ions, thiols and the total protein were determined spectrophotometrically using PAR and DTNB assays[6,7] or by UV range measurements at 220 nm. Accordingly, MT-1e, MT-2 and MT-3 contained 6.95 ± 0.11, 7.12 ± 0.07 and 7.06 ± 0.10 Zn(II) ions per molecule, respectively. MT-1e sample was used for the CD measurements.

General procedures

Stock solutions of the ligands were prepared in anhydrous DMSO (≥99.9%), as well as further diluted solutions. Concentration of the ligands were confirmed by titration of a Cu(II) solution of known concentration in HEPES buffer 100 mM, pH 7.4/20% DMSO (gtsm), 40% DMSO (atsm) monitored by UV-Visible Spectroscopy. A stock solution of Cu(II) (100 mM) was prepared by dissolving the salt in Milli-Q water. Its concentration was verified by UV-Vis absorption spectroscopy through the Cu(II) d-d band at 780 nm (ε = 12 $M^{-1}cm^{-1}$). A stock solution of Cu(I) (3 mM) was prepared in CH_3CN under saturated argon atmosphere. A stock solution of Zn(II) (100 mM) was obtained by dissolving the salt in Milli-Q water. A stock solution of HEPES buffer (500 mM, pH 7.4) was prepared by dissolving HEPES (free acid) in Milli-Q water, adjusting the pH with a 5 M solution of NaOH. A Stock solution GSH (100 mM) was freshly prepared daily by dissolving the powder into a 72.4 mM solution of HCl in Milli-Q water. A stock solution of sodium ascorbate (100 mM) was freshly prepared daily in Milli-Q water. Spin-trap POBN stock solution (500 mM) was prepared in 500 mM PB, pH 7.4.

Reaction mixtures

For all the studies deionized Milli-Q water (18 MW) was employed. All the reactions monitored via absorbance spectroscopy and circular dichroism were carried out in the presence of HEPES buffer 100 mM, pH 7.4. Stock solutions of all the reactants were mixed inside quartz cuvettes (used for spectroscopic characterization) to obtain the final concentration desired and the reactions monitored over time. Reactions were carried out at RT, in the presence of O_2.
For Low T EPR experiments all samples were supplemented by 10 % v/v glycerol to ensure homogeneous sample distribution. Reaction mixtures were immediately transferred in to a 4 mm outer diameter quartz tubes (Wilmad-Labglass) and immediately freeze-quenched with liquid nitrogen prior to their introduction in to the precooled cavity.
For EPR spin-trap experiments POBN was used as primary spin-trap and ~5 % of DMSO (from the ligand stock solution) was present in all samples and used as secondary spin-trap to enhance the EPR signal. Fe(III)-PT, generated by mixing a stock solution of Fe(III) and PT in TRIS 50 mM, pH 7.5, was incubated for 30 min at 40° C before its use. Reaction mixtures (containing POBN) were immediately transferred in to a EPR capillary after addition of GSH or GSH/Zn_7MT-1.

Spectrophotometric measurements

For absorption spectroscopy a single-beam Agilent Cary 60 UV-Vis spectrophotometer was employed. Measurements were performed in the 800-200 nm spectral range with a 50 µl 10 mm quartz cuvette with a final volume of 100 µl. The obtained spectra are express as absorbance.

For circular dichroism a Jasco J-810 Spectropolarimeter was employed. CD spectra were recorded in the spectral range 400-250 nm with a scanning speed of 50 nm/min in a 500 µl 10 mm quartz cuvette with a final volume of 500 µl. The obtained spectra are express as ellipticity (mdeg).
Both spin trapping investigations and low temperature EPR experiments were acquired on an EMX X-band spectrometer (EMXplus from Bruker Biopsin GmbH, Germany), equipped with a high sensitivity resonator (4119HS-W1, Bruker). The g factor was calibrated in the experimental conditions using the Bruker strong pitch (g = 2.0028). Low temperatures were achieved using continuous flow liquid nitrogen cryostat. Principal spectrometer settings for spin-trapping: center field: 3510 G, sweep width: 80 G, microwave power: 4.5 mW, modulation amplitude: 1 G, gain: 50 dB, conversion time: ca 250 ms, time constant: ca. 80 ms, 1 scan/720 pts/180sec. Principal spectrometer settings for low temperature experiments: center field: 3100 G, sweep width: 1500 G, microwave power: 0.1 mW, modulation amplitude: 5 G, gain: 30 dB, conversion time: ca. 300 ms, time constant: ca. 80 ms, 1 scan/1500 pts/300sec. 1−10 scans were accumulated to achieve reasonable signal-to-noise ratio.
ESI-MS measurements were recorded in a MicroTOF-Q (Brucker Daltonics GmbH, Bremen, Germany) instrument equipped with an electrospray ionization source (ESI) in positive mode, interfaced with a Series 1200 HPLC Agilent pump, equipped with an autosampler, all of which were controlled by the Compass Software. Conditions used were those optimized for metal-metallothionein samples analysis: 40 µL min^{-1} flow rate, in a spectra collection range 800-2500 m/z. The carrier buffer was a 5:95 mixture of acetonitrile : 15 mM ammonium acetate/ammonia (pH 7.0).

References

[1] N. Romero-Isart, L. T. Jensen, O. Zerbe, D. R. Winge and M. Vašák, *J. Biol. Chem.*, 2002, 277, 37023.

[2] N. Cols, N. Romero-Isart, M. Capdevila, B. Oliva, P. Gonzalez-Duarte, R. Gonzalez-Duarte and S. Atrian, *J. Inorg. Biochem.*, 1997, 68, 157.

[3] A. Drozd, D. Wojewska, M.D. Peris-Díaz, P. Jakimowicz, A. Krężel, *Metallomics*, 2018, *10*, 595.

[4] A. Krężel, W. Maret, *J. Am. Chem. Soc.,* 2007, *129*, 109116.

[5] A. Krężel, R. Latajka, G. D. Bujacz, W. Bal, *Inorg. Chem.,* 2003, *42*, 1994.

[6] A. Kocyła, A. Pomorski, A. Krężel, *J. Inorg. Biochem.,* 2015, *152*, 82.

[7] P. Eyer, F. Worek, D. Kiderlen, G. Sinko, A. Stuglin, V. Simeon-Rudolf, E. Reiner, *Anal. Biochem*., 2003, *312*, 224.

Cu(II) titration experiments (absorbance spectroscopy)

Cu(II) titration experiments on the different TSCs and bTSCs were carried out in order to elucidate the stoichiometry of the metal-complex formed under the experimental conditions of the studied reactions. In all cases a steady increase in intensity of the absorption bands of the formed complex were detected, along with the decrease in intensity of those of the free ligand (Figure S1-5). Binding curves were obtained by plotting the maximum of absorbance of the formed complex (λ_{max}) versus Cu(II)/L ratio. Cu(II) complexes with a binding stoichiometry of 1:1 were obtained for all the ligands. In case of the Dp44mT, both the formation a 1:2 (Cu(II):2L) and 1:1 (Cu(II):L) were observed.

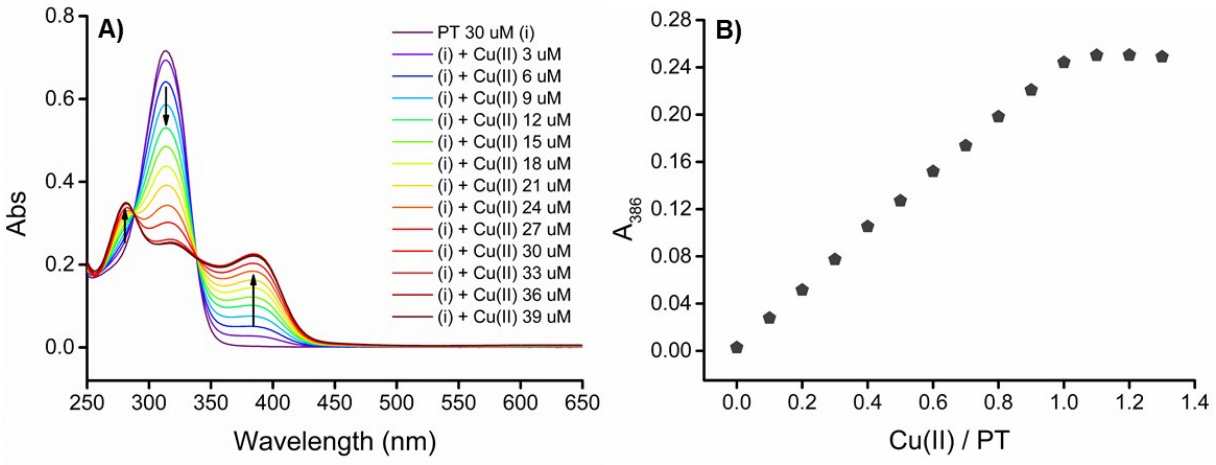

Fig. S1 Cu(II) titration to determine the binding stoichiometry Cu(II) / PT.

A) UV-Vis spectra; B) corresponding binding curve at λ_{max} = 382 nm.

Experimental conditions: A 30 μM solution of PT in HEPES buffer 100 mM, pH 7.4, was titrated with 1 μL aliquots of a 300 μM Cu(II) stock solution.

Cu(II)-PT: λ_{max} = 382 nm, λ_{max} = 318 nm, λ_{max} = 280 nm, isosbestic points at λ = 338 nm, λ = 287 nm

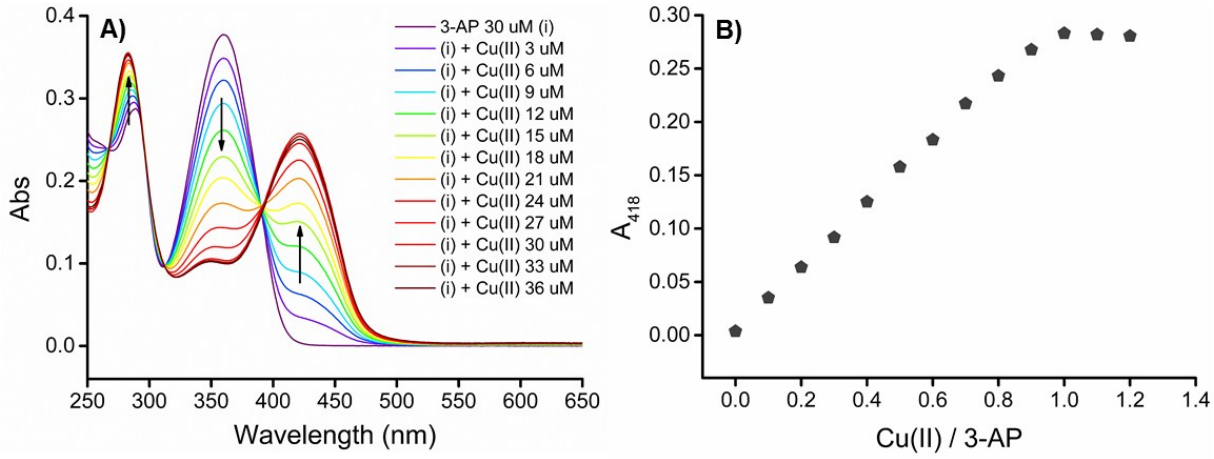

Fig. S2 Cu(II) titration to determine the binding stoichiometry Cu(II) / 3-AP.

A) UV-Vis spectra; B) corresponding binding curve at λ_{max} = 418 nm.

Experimental conditions: A 30 μM solution of 3-AP in HEPES buffer 100 mM, pH 7.4, was titrated with 1 μL aliquots of a 300 μM Cu(II) stock solution.

Cu(II)-3-AP: λ_{max} = 418 nm, λ_{max} = 349 nm, λ_{max} = 283 nm, isosbestic points at λ = 393 nm, λ = 311 nm, λ = 366 nm

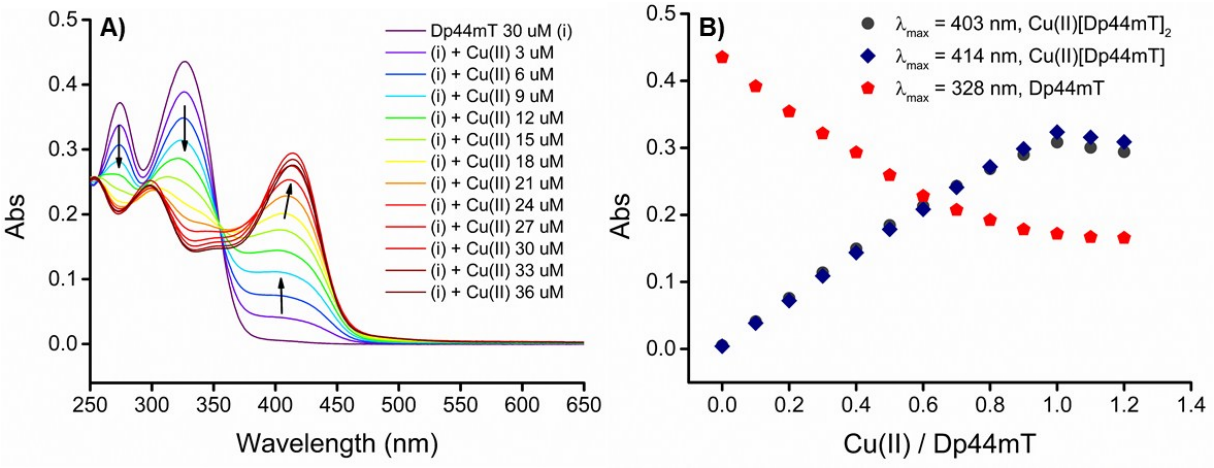

Fig. S3 Cu(II) titration to determine the binding stoichiometry Cu(II) / Dp44mT.

A) UV-Vis spectra; B) corresponding binding curves at λ_{max} = 411 nm (CT band 1:1 complex Cu(II)[Dp44mT]), λ_{max} = 402 nm (CT band 1:2 complex Cu(II)$[Dp44mT]_2$) and λ_{max} = 328 nm (free Dp44mT).

Experimental conditions: A 30 μM solution of Dp44mT in HEPES buffer 100 mM, pH 7.4, was titrated with 1 μL aliquots of a 300 μM Cu(II) stock solution.

The appearance of two distinct isosbestic points (λ_1 = 354 nm, until the addition of 0.5 equivalents with respect to Dp44mT, λ_2 = 389 nm, from the addition of 0.6 eq with respect to Dp44mT) suggest the formation of two species, Cu(II)$[Dp44mT]_2$ and Cu(II)[Dp44mT] with a 2:1 and 1:1 stoichiometry (Dp44mT : Cu(II)) respectively.

Cu(II)-$[Dp44mT]_2$: λ_{max} = 403 nm, λ_{max} = 310 nm, λ_{max} = 304 nm

Cu(II)-Dp44mT: λ_{max} = 414 nm, λ_{max} = 298 nm, λ_{max} = 253 nm

Reactivity of the Cu(II)-TSC complexes with GSH

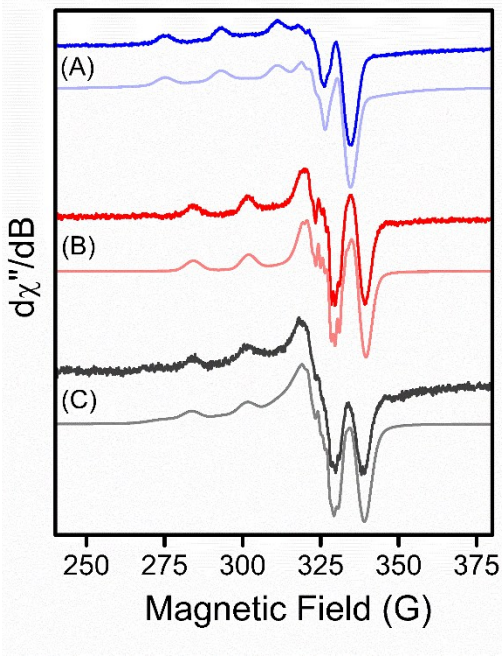

Fig. S4 EPR spectra and corresponding simulation of snap-frozen solutions of the (A) Cu(II)-PT complex (blue lines), (B) after the addition of GSH (red lines) and (C) after the addition of Zn_7MT-1 (grey line).

Experimental conditions: 1 mM PT, 900 μM Cu(II), 3 mM GSH or 200 μM Zn_7MT-1 (ratio PT/Cu(II)/Zn_7MT-1 1:0.9:0.2), HEPES Buffer 100 mM, pH 7.4 and T = 100 K. All samples were supplemented by 10 % v/v glycerol. Simulation parameters are given in Table S1. The simulations were achieved with Easyspin Toolbox under Matlab environment (Stoll et al JMR, 178(1), 42-55, 2006). A broad Cu(II) EPR fingerprint was implemented to the simulation of (a) and (c) to account for the observed baseline, arising from the sample solubility limit.

Table S1: Principal EPR simulations parameters.[a,b]

Species	PT,Cu(II) (1:0.9) (i)[c]	(i) + GSH	(i) +Zn_7MT-1[b]
$g_{//}$	2.205	2.142	2.147
$A_{//}$ (Cu(II)) (MHz)	544	520	515

[a] field strain and linewidth parameters were used to account for the experimental line-broadening.

[b] Isotropic superhyperfine coupling constants for accounting for 2 nitrogen atoms of 40±5 MHz were implemented to the computation.

[c] broad Cu(II) EPR fingerprint was implemented to the simulation to account for the observed baseline, arising from the solubility limit of our sample.

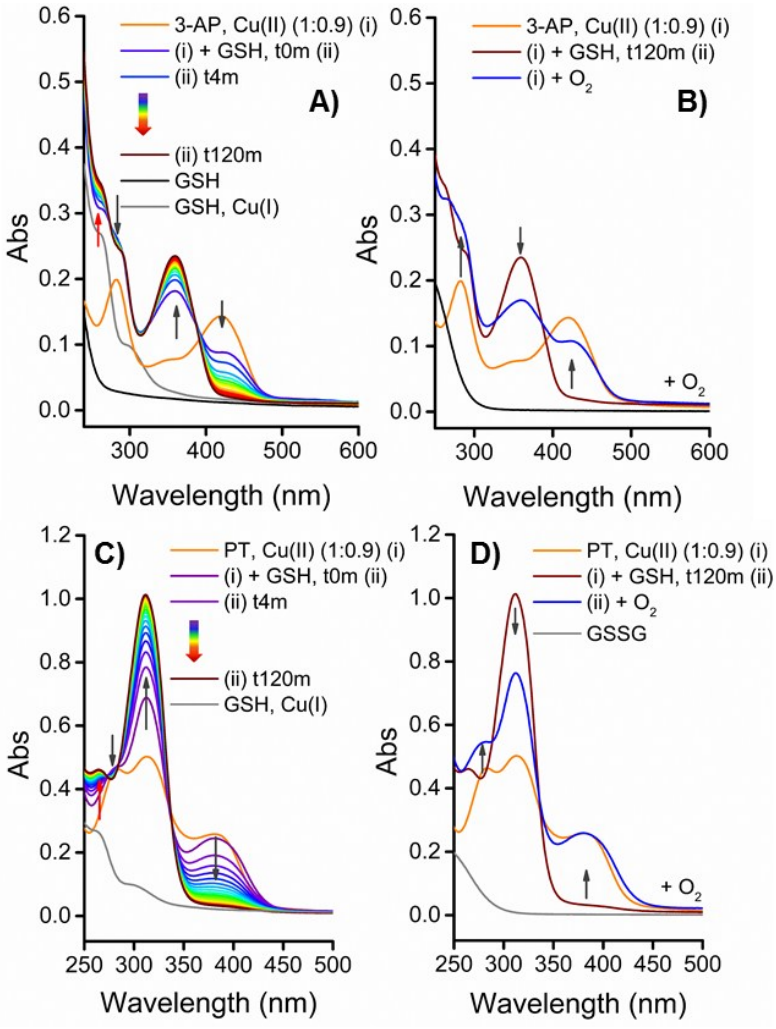

Fig. S5 Reactivity of Cu(II)-3-AP/PT complexes with GSH under anaerobic conditions (A,C) and after bubbling O_2 through the solution (B, D).

A), C) UV-Vis spectra for the reaction between Cu(II)-3-AP/PT and 1 mM GSH under anaerobic conditions. The reactions were monitored over time from t_0 min after GSH addition to the preformed Cu(II)-3-AP/PT complexes (ratio 3-AP/PT:Cu(II), 1:0.9) to t_{120} min, collecting each intermediate spectrum at 4 min intervals. The dark grey arrows indicate the changes observed in the spectra after GSH addition to the preformed Cu(II)-3AP/PT complexes (orange lines) i.e the disappearance of the CT bands of the ternary adduct [TSC-Cu(II)-GSH] (λ_{max} (3-AP) = 425 nm, λ_{max} (PT) = 386 nm), and appearance of UV band of the free ligand (λ_{max} (3-AP) = 359 nm, λ_{max} (PT) = 313 nm). The red arrows indicate the appearance of characteristic CT band of the Cu(I)-GSH complex at λ_{max} = 265 nm. B), D) Corresponding spectra (blue lines) obtained after bubbling O_2 through the solution. The dark grey arrows indicate the changes from the wine red spectrum (Cu(II)-3-AP/PT + GSH, t120m in anaerobic conditions) to the blue spectrum.

Experimental conditions: To a solution of 15 μM 3-AP, 27 μM Cu(I) (A) and 30 μM PT and 27 μM Cu(I) (ratio TSC:Cu(I), 1:0.9) in 100 mM HEPES buffer, pH 7.4, 5 μL of 200 mM stock solution of GSH were respectively added, to obtain a final concentration of GSH of 1 mM. The reaction mixtures were prepared under saturated argon atmosphere in a screw cap cell cuvette equipped with septum. Upon Cu(I) addition to the ligand solution the characteristic UV spectra of the Cu(II)-3-AP/PT complexes were immediately detected.

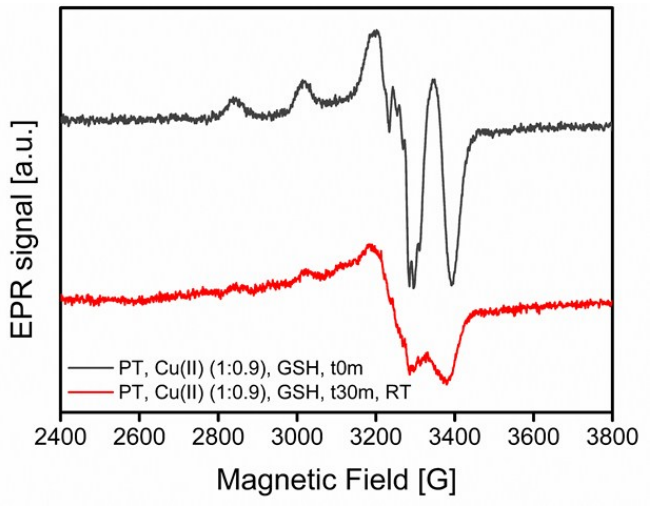

Fig. S6 Reactivity of Cu(II)-PT complex with GSH (detection of the ternary adduct [PT-Cu(II)-GSH]).

EPR spectra of the snap-frozen solution of Cu(II)-PT after the addition of GSH (dark grey line); room temperature EPR spectra at t_{30} min after GSH addition to Cu(II)-PT complex (red line)

Experimental conditions : To a solution of 1 mM PT and 900 μM Cu(II) (100 μL) (ratio PT:Cu(II), 1:0.9) in HEPES buffer 100 mM, pH 7.4, 3 μL of a 100 mM GSH stock solution were added to obtain a final concentration of 3 mM.

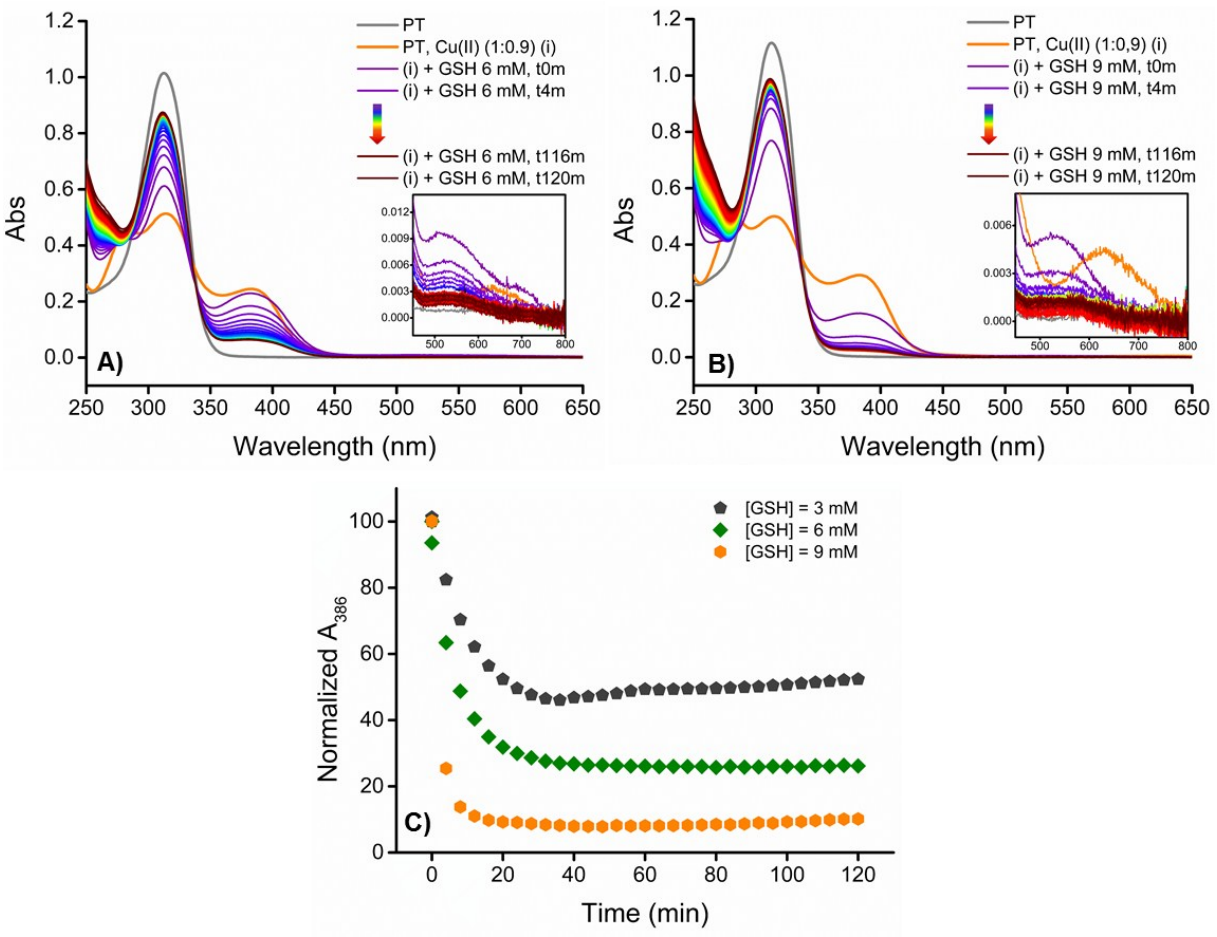

Fig. S7 Concentration dependence of the Cu(II)-PT complex reactivity with GSH.

A) UV-Vis spectra for the reaction between Cu(II)-PT and 6 mM GSH B) 9 mM GSH. The reactions were monitored over time from t_0 min after GSH addition to the preformed Cu(II)-PT complex (ratio PT:Cu(II), 1:0.9) to t_{120} min, collecting each intermediate spectrum at 4 min intervals. Insets in Figure A), B), refer to the Vis region of the spectra 450-800 nm. C) Corresponding experimental kinetics for the reactions of the Cu(II)-PT complex with different concentrations of GSH, respectively 3 mM (dark grey kinetic), 6 mM (dark green kinetic), 9 mM (orange kinetic): normalized absorbance at λ_{max} = 386 nm (CT band of the ternary complex [PT-Cu(II)-GSH]) versus time.

Experimental conditions: To a solution of 30 μM PT and 27 μM Cu(II) (ratio PT:Cu(II), 1:0.9) in HEPES buffer 100 mM, pH 7.4, 6 μl (A) and 9 μl (B) of a stock solution 100 mM of GSH were respectively added, to obtain a final concentration of GSH of 6 mM (A) and 9 mM (B).

Reactivity of the Cu(II)-TSC complexes with Zn_7MT-1

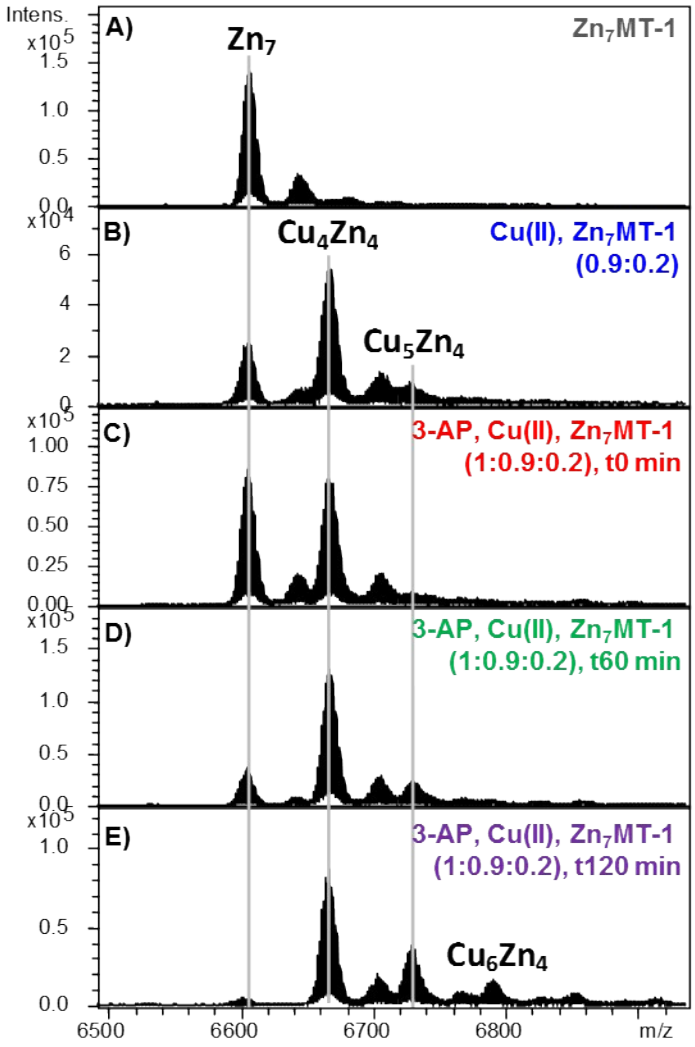

Fig. S8 Reactivity of Cu(II)-3-AP with Zn_7MT-1. Deconvoluted ESI-MS spectra (A) of Zn_7MT-1, (B) Cu(II)/Zn_7MT-1, 0.9:0.2, (C) 3-AP/Cu(II)/Zn_7MT-1, 1:0.9:0.2 (t_0 min from the addition of Zn_7MT-1 to the preformed Cu(II)-3-AP complex), AP/Cu(II)/Zn_7MT-1, 1:0.9:0.2 (t_{60} min from the addition of Zn_7MT-1 to the preformed Cu(II)-3-AP complex), 3-AP/Cu(II)/Zn_7MT-1, 1:0.9:0.2 (t_{120} min from the addition of Zn_7MT-1 to the preformed Cu(II)-3-AP complex). Experimental conditions: 50 µM 3-AP, 45 µM Cu(II) , 10 µM Zn_7MT-1 (ratio 3-AP:Cu(II):Zn_7MT-1, 1:0.9:0.2), 50 mM ammonium acetate, pH 7.4.
The main peak in A) of m/z 6610 has the mass expected for Zn_7MT-1 at neutral pH; the main peak at m/z 6671 in B, C, D, E) corresponds to a substitution of three Zn(II) ions with four Cu(I) ions; the peaks at m/z 6732 and 6792 correspond to a substitution of three Zn(II) ions with respectively five and six Cu(I) ions.

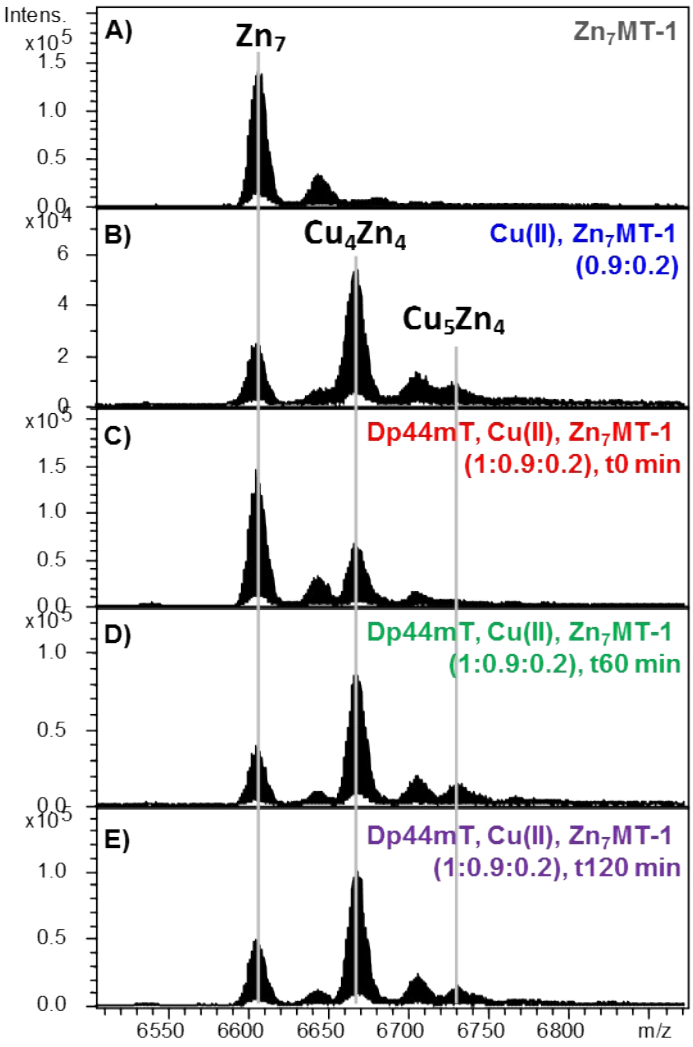

Fig. S9 Reactivity of Cu(II)-Dp44mT with Zn_7MT-1. Deconvoluted ESI-MS spectra (A) of Zn_7MT-1, (B) Cu(II)/Zn_7MT-1, 0.9:0.2, (C) Dp44mT/Cu(II)/Zn_7MT-1, 1:0.9:0.2 (t_0 min from the addition of Zn_7MT-1 to the preformed Cu(II)-Dp44mT complex), Dp44mT/Cu(II)/Zn_7MT-1, 1:0.9:0.2 (t_{60} min from the addition of Zn_7MT-1 to the preformed Cu(II)-Dp44mT complex), Dp44mT/Cu(II)/Zn_7MT-1, 1:0.9:0.2 (t_{120} min from the addition of Zn_7MT-1 to the preformed Cu(II)-Dp44mT complex). Experimental conditions: 50 µM Dp44mT, 45 µM Cu(II) , 10 µM Zn_7MT-1 (ratio 3-AP:Cu(II):Zn_7MT-1, 1:0.9:0.2), 50 mM ammonium acetate, pH 7.4.

The main peak in A) of m/z 6610 has the mass expected for Zn_7MT-1 at neutral pH; the main peak in B, C, D, E) at m/z 6671 corresponds to a substitution of three Zn(II) ions with four Cu(I) ions; the peak at m/z 6732, correspond to a substitution of three Zn(II) ions with respectively five and six Cu(I) ions.

Reactivity of the Cu(II)-TSC complexes with Zn_7MT-1 and GSH

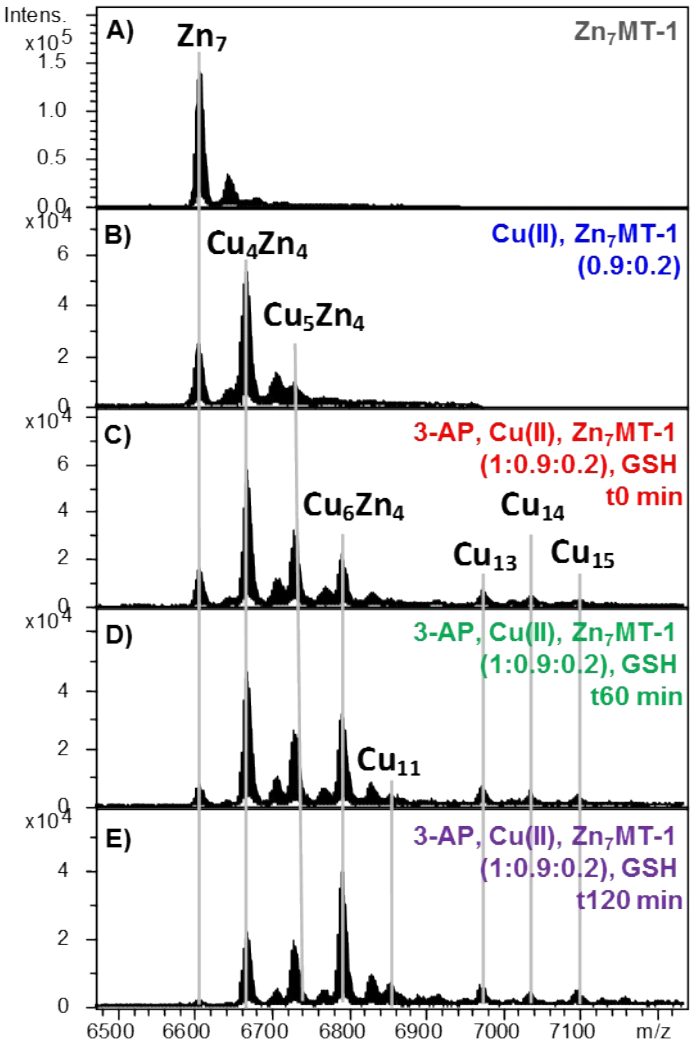

Fig. S10 Reactivity of Cu(II)-3-AP with Zn_7MT-1/GSH. Deconvoluted ESI-MS spectra (A) of Zn_7MT-1, (B) Cu(II)/Zn_7MT-1, 0.9:0.2, (C) 3-AP/Cu(II)/Zn_7MT-1, 1:0.9:0.2, GSH (t_0 min from the addition of Zn_7MT-1/GSH to the preformed Cu(II)-3-AP complex), AP/Cu(II)/Zn_7MT-1, 1:0.9:0.2, GSH (t_{60} min from the addition of Zn_7MT-1/GSH to the preformed Cu(II)-3-AP complex), 3-AP/Cu(II)/Zn_7MT-1, 1:0.9:0.2, GSH (t_{120} min from the addition of Zn_7MT-1/GSH to the preformed Cu(II)-3-AP complex). Experimental conditions: 50 µM 3-AP, 45 µM Cu(II) , 10 µM Zn_7MT-1 (ratio 3-AP:Cu(II):Zn_7MT-1, 1:0.9:0.2), 3 mM GSH, 50 mM ammonium acetate, pH 7.4.

The main peak in A) of m/z 6610 has the mass expected for Zn_7MT-1 at neutral pH; the main peak at m/z 6671 in B, C, D, E) corresponds to a substitution of three Zn(II) ions with four Cu(I) ions; the peaks at m/z 6732 and 6792 correspond to a substitution of three Zn(II) ions with respectively five and six Cu(I) ions. The peaks at m/z 6860, 6880, 7040 and 7100 correspond to a substitution of seven Zn(II) ions with respectively eleven, thirteen, fourteen, fifteen Cu ions.

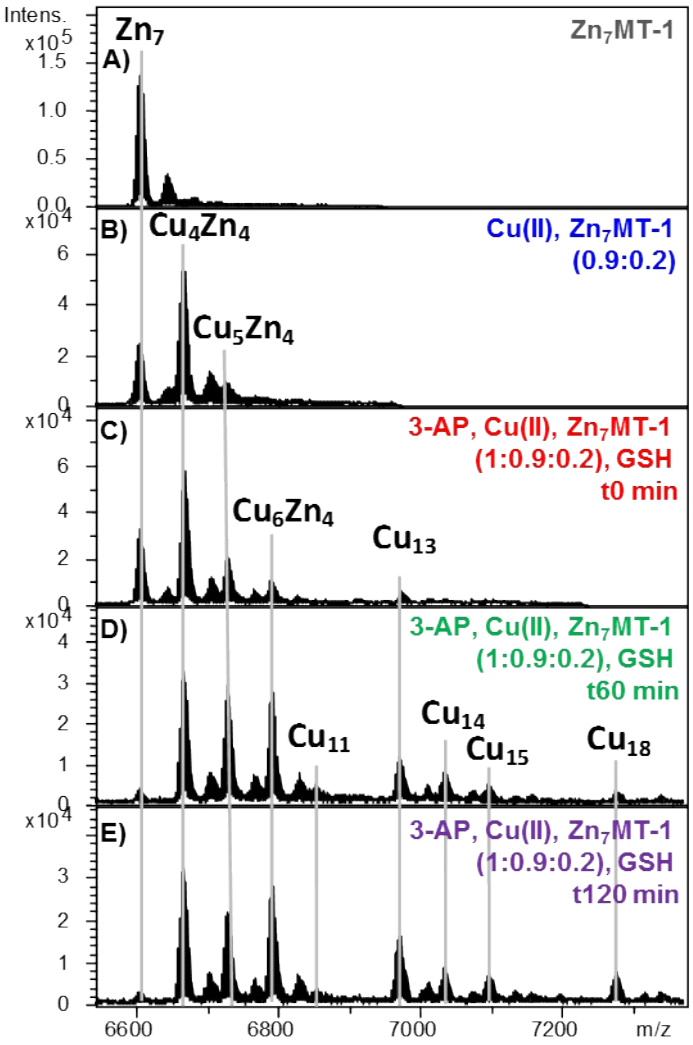

Fig. S11 Reactivity of Cu(II)-Dp44mT with Zn_7MT-1. Deconvoluted ESI-MS spectra (A) of Zn_7MT-1, (B) Cu(II)/Zn_7MT-1, 0.9:0.2, (C) Dp44mT/Cu(II)/Zn_7MT-1, 1:0.9:0.2, GSH (t_0 min from the addition of Zn_7MT-1/GSH to the preformed Cu(II)-Dp44mT complex), Dp44mT/Cu(II)/Zn_7MT-1, 1:0.9:0.2, GSH (t_{60} min from the addition of Zn_7MT-1/GSH to the preformed Cu(II)-Dp44mT complex), Dp44mT/Cu(II)/Zn_7MT-1, 1:0.9:0.2, GSH (t_{120} min from the addition of Zn_7MT-1/GSH to the preformed Cu(II)-Dp44mT complex). Experimental conditions: 50 µM Dp44mT, 45 µM Cu(II) , 10 µM Zn_7MT-1 (ratio Dp44mT:Cu(II):Zn_7MT-1, 1:0.9:0.2), 3 mM GSH, 50 mM ammonium acetate, pH 7.4.
The main peak in A) of m/z 6610 has the mass expected for Zn_7MT-1 at neutral pH; the main peak in B, C, D) at m/z 6671 corresponds to a substitution of three Zn(II) ions with four Cu(I) ions; the peaks at m/z 6732 and 6792, correspond to a substitution of three Zn(II) ions with respectively five and six Cu(I) ions. The peaks at m/z 6860, 6880, 7040, 7100 and 7280 correspond to a substitution of seven Zn(II) ions with respectively eleven, thirteen, fourteen, fifteen and eighteen Cu ions.

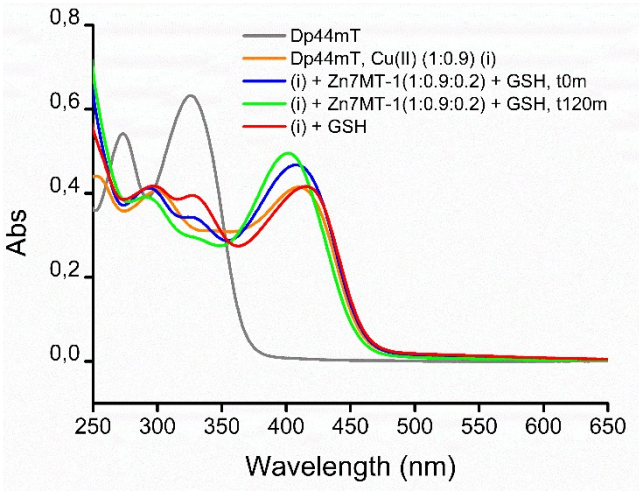

Fig. S12 Comparison of the spectra for the reaction of Cu(II)-Dp44mT with GSH (red line) and for the reaction of Cu(II)-Dp44mT with GSH and Zn_7MT-1 (blue line, t_0 min, green line, t_{120} min).

Experimental conditions: Dp44mT 30 μM (grey line), Dp44mT 30 μM, Cu(II) 27 μM (1:0.9) (orange line), Dp44mT 30 μM, Cu(II) 27 μM + Zn_7MT-1 6 μM (1:0.9:0.2) + GSH 3 mM, spectra recorded at t_0 min from Zn_7MT-1 and GSH addition to the preformed Cu(II)-Dp44mT complex (blue line), Dp44mT 30 μM, Cu(II) 27 μM + Zn_7MT-1 6 μM (1:0.9:0.2) + GSH 3 mM, spectra recorded at t_{120} min from Zn_7MT-1 and GSH addition to the preformed Cu(II)-Dp44mT complex (green line), Dp44mT 30 μM, Cu(II) 27 μM (1:0.9) + GSH 3 mM, spectrum recorded at t_0 min from GSH addition to the preformed Cu(II)-Dp44mT complex (red line).

Reactivity of the Cu(II)-TSC complexes with Zn_7MT and GSH: comparison among different MT isoforms

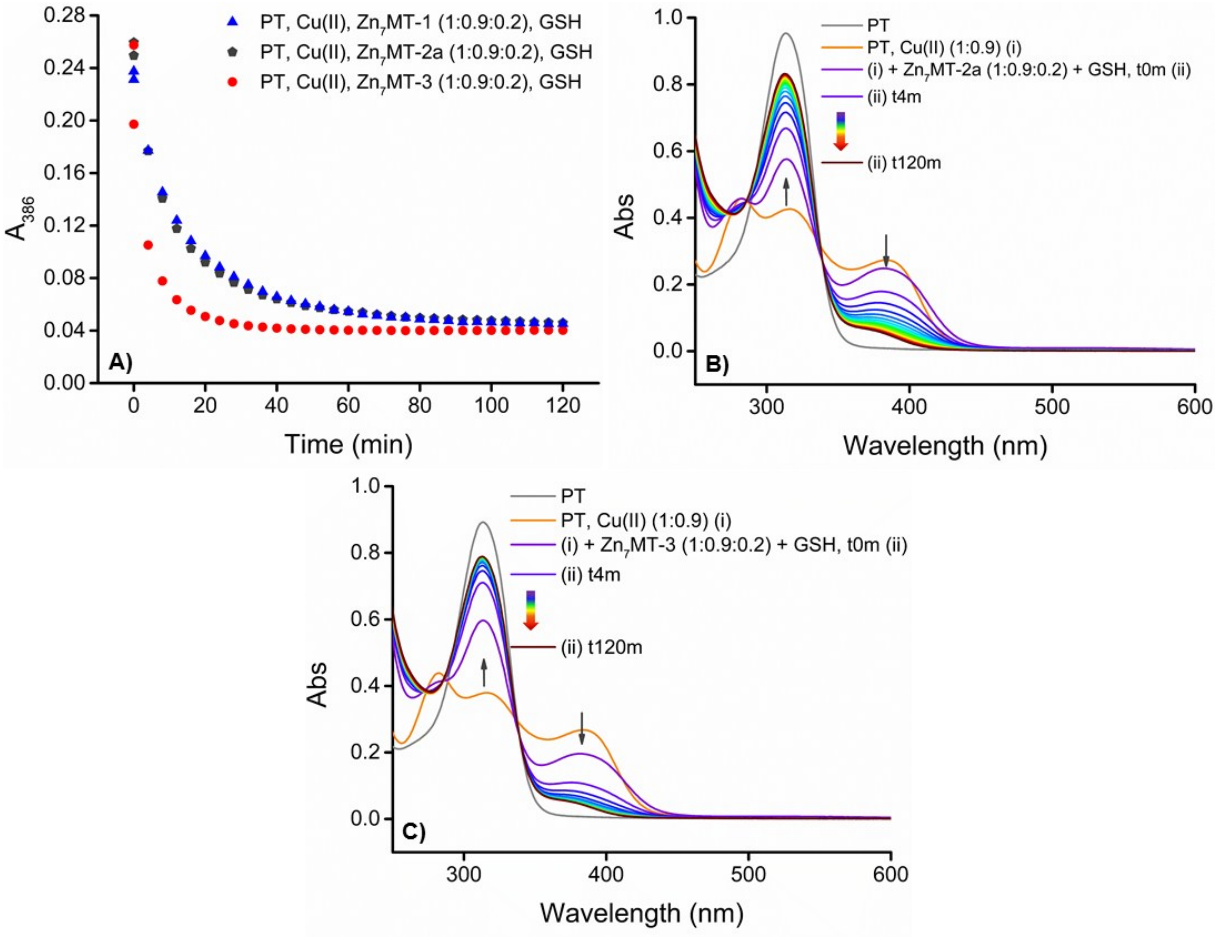

Fig. S13 Reactivity of Cu(II)-PT complex with GSH and different isoforms of MT (Zn_7MT-1, Zn_7MT-2a, Zn_7MT-3).

A) Experimental kinetics for the reactions of Cu(II)-PT complex with different isoforms of Zn_7MT in the presence of 3 mM GSH: Zn_7MT-1 isoform (blue profile), Zn_7MT-2a isoform (grey profile), Zn_7MT-3 isoform (red profile). The absorbance at λ_{max} = 386 nm (CT band of the ternary complex [PT-Cu(II)-GSH]) is reported versus time. B), C) Corresponding UV-Vis spectra for the reaction with GSH/Zn_7MT-2a B) GSH/Zn_7MT-3 (C) monitored over time after GSH/ addition to the preformed Cu(II)-PT complex (for the reaction with Zn_7MT-1 , see Fig. 7B).

Experimental conditions: To a solution of 30 μM 3-AP and 27 μM Cu(II) (ratio PT:Cu(II), 1:0.9) in HEPES buffer 100 mM, pH 7.4, GSH at 3 mM concentration and Zn_7MT-1/Zn_7MT-2a/Zn_7MT-3 at 6 μM were respectively added and the reaction monitored over time for 120 min, collecting each intermediate spectrum at 4 min intervals.

The direction of the arrows refer to the direction of the changes of the absorbance bands from the initial spectrum of the preformed complex Cu(II)-PT after GSH/Zn_7MT addition (disappearance of the CT band of the ternary adduct [PT-Cu(II)-GSH] (λ_{max} = 386 nm) and re-appearance of the UV band of the free ligand PT (λ_{max} = 313 nm)).

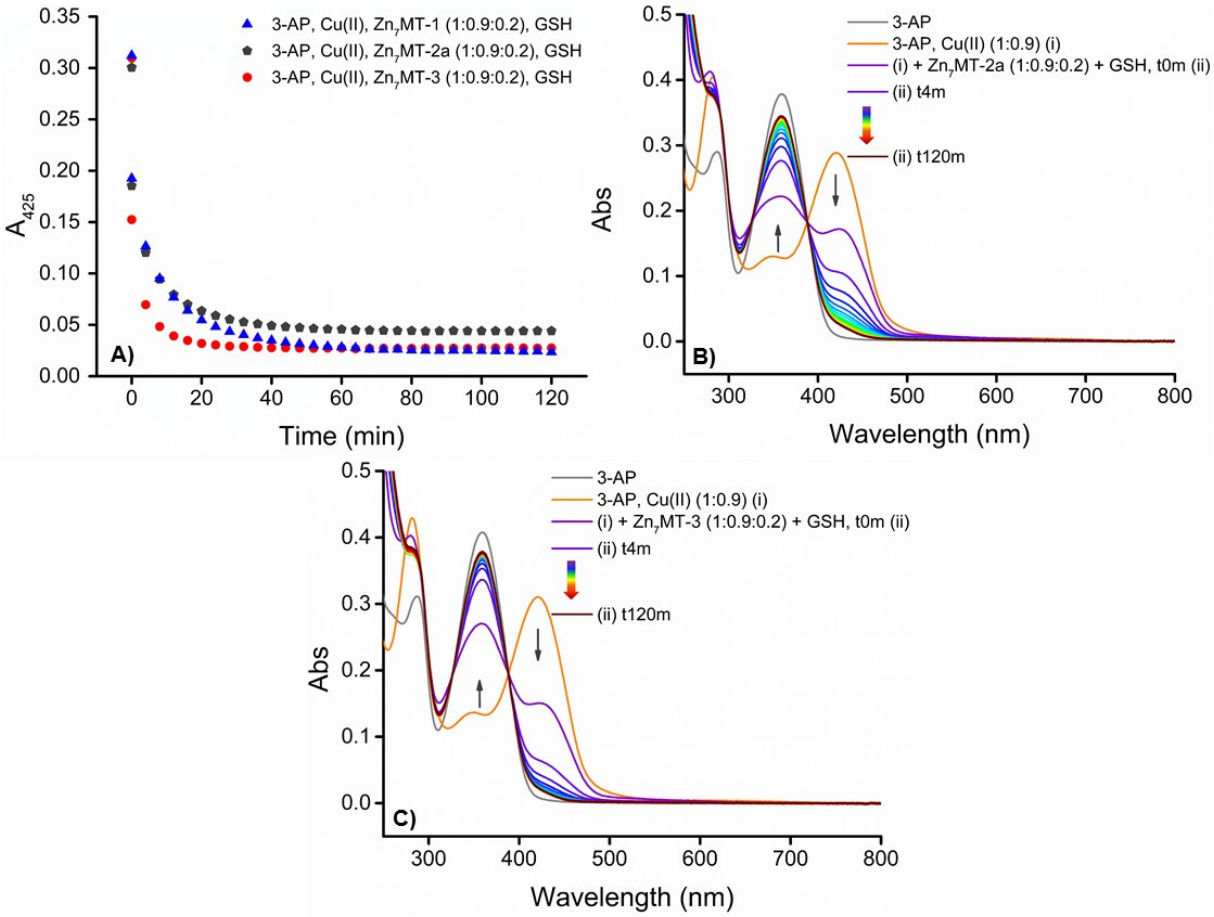

Fig. S14 Reactivity of Cu(II)-3-AP complex with GSH and different isoforms of MT (Zn_7MT-1, Zn_7MT-2a, Zn_7MT-3).

A) Experimental kinetics for the reactions of the Cu(II)-3-AP complex with different isoforms of Zn_7MT in the presence of 3 mM GSH: Zn_7MT-1 isoform (blue profile), Zn_7MT-2a isoform (grey profile), Zn_7MT-3 isoform (red profile). The absorbance at λ_{max} = 424 nm (CT band of the ternary complex [3-AP-Cu(II)-GSH]) is reported versus time. B), C) Corresponding UV-Vis spectra for the reaction with GSH/Zn_7MT-2a B) GSH/Zn_7MT-3 (C) monitored over time after GSH/Zn_7MT addition to the preformed Cu(II)-3-AP complex (for the reaction with Zn_7MT-1 , see Fig. 7C).

Experimental conditions: To a solution of 30 μM 3-AP and 27 μM Cu(II) (ratio PT:Cu(II), 1:0.9) in HEPES buffer 100 mM, pH 7.4, GSH and Zn_7MT-1/Zn_7MT-2a/Zn_7MT-3 at 3 mM and 6 μM concentration respectively were added and the reaction monitored over time for 120 min, collecting each intermediate spectrum at 4 min intervals.

The direction of the arrows refer to the direction of the changes of the absorbance bands from the initial spectrum of the preformed complex Cu(II)-3-AP after GSH/Zn_7MT addition (disappearance of the CT band of the ternary adduct [3-AP-Cu(II)-GSH] (λ_{max} = 424 nm) and re-appearance of the UV band of the free ligand 3-AP (λ_{max} = 359 nm)).

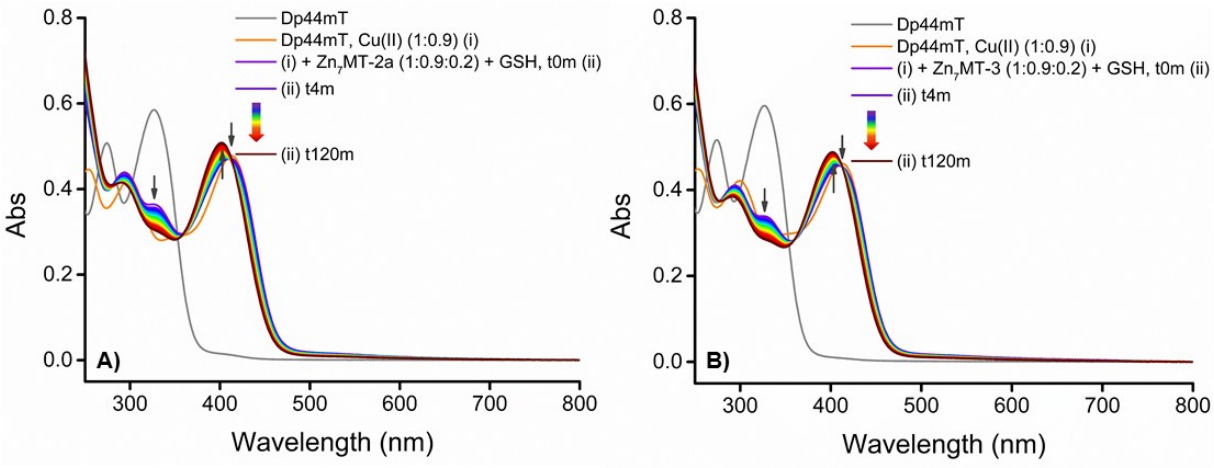

Fig. S15 Reactivity of Cu(II)-Dp44mT complex with GSH and different isoforms of MT (Zn_7MT-1, Zn_7MT-2a, Zn_7MT-3).

A), B) UV-Vis spectra for the reaction of Cu(II)-Dp44mT with GSH/Zn_7MT-2a (A) GSH/Zn_7MT-3 (B) monitored over time after GSH/Zn_7MT addition to the preformed Cu(II)-3-AP complex (for the reaction with Zn_7MT-1 , see Fig. 7D).

Experimental conditions: To a solution of 30 μM Dp44mT and 27 μM Cu(II) (ratio PT:Cu(II), 1:0.9) in HEPES buffer 100 mM, pH 7.4, GSH and Zn_7MT-2a/Zn_7MT-3 at 3 mM and 6 μM concentration respectively were added and the reaction monitored over time for 120 min, collecting each intermediate spectrum at 4 min intervals.
The direction of the arrows refer to the direction of the changes of the absorbance bands from the initial spectrum of the preformed complex Cu(II)-3-AP after GSH/Zn_7MT addition (disappearance of the CT bands of the ternary adduct [Dp44mT-Cu(II)-GSH/Zn_7MT-1] and appearance of the CT band Zn(II)-$Dp44mT_2$ (λ_{max} = 398 nm)).

Table S2:

Table summarizing the $t_{1/2}$ (min) values for the reactions of Cu(II)-PT and Cu(II)-3-AP with GSH and Zn_7MT-1/Zn_7MT-2a/Zn_7MT-3. $t_{1/2}$ values were calculated from the experimental kinetics of disappearance of the of CT bands of the [PT/3-AP- Cu(II)-GSH] complexes (λ_{max} [PT-Cu(II)-GSH] = 386 nm, λ_{max} [3-AP-Cu(II)-GSH] = 424 nm). Experimental kinetics were fitted with a 1st order exponential equation y = W*exp(-k*x)+A.

Reaction	$t_{1/2}$ (min)
Cu(II)-PT + Zn_7MT-1 + GSH	10.4
Cu(II)-PT + Zn_7MT-2a + GSH	8.2
Cu(II)-PT + Zn_7MT-3 + GSH	3.1
Cu(II)-3-AP + Zn_7MT-1 + GSH	5.0
Cu(II)-3-AP + Zn_7MT-2a + GSH	3.8
Cu(II)-3-AP + Zn_7MT-3 + GSH	1.9

Zn(II) titration experiments (absorbance spectroscopy)

Zn(II) titration experiments on the different TSCs and bTSCs were carried out in order to characterize by absorbance the Zn(II) binding behavior to the ligands under the experimental conditions of the studied reactions. (Figure S9-12) Under our conditions only for the ligand Dp44mT a complex with a define stoichiometry 1:2 metal-ligand was observed, shown by the complete conversion of the ligand into the Zn(II)[Dp44mT]$_2$ complex with a single distinct isosbestic point at 354 nm.
Absorption bands of the formed complexes were detected in the region 360-440 nm. Binding curves were obtained by plotting the maximum of absorbance of the formed complex (λ_{max}) versus [Zn(II)]/ [L] ratio.

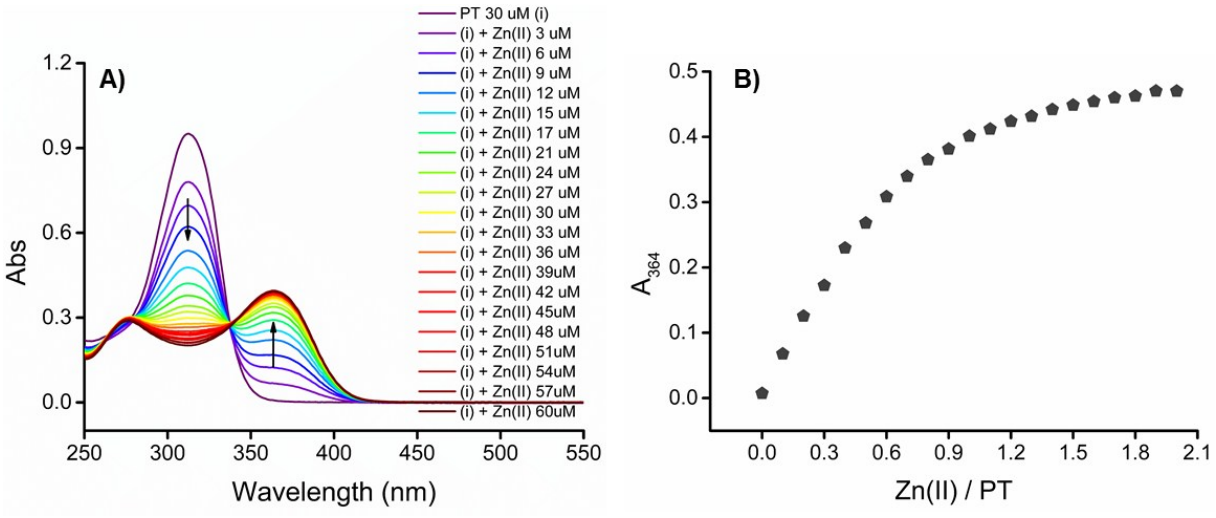

Fig. S16 Zn(II) titration of the ligand PT.

A) UV-Vis spectra; B) corresponding binding curve at λ_{max} = 364 nm.

Experimental conditions: A 30 μM solution of PT in 100 mM HEPES buffer pH 7.4, was titrated with 1 μL aliquots of a 300 μM Zn(II) stock solution.

Zn(II) addition to the PT solution induced the appearance of two new bands in the UV region, respectively at λ_{max} = 364 nm and λ_{max} = 275 nm, along with the disappearance of the free ligand band at 313 nm. (isosbestic point, λ = 337 nm).

Zn(II)-PT: λ_{max} = 364 nm, λ_{max} = 275 nm

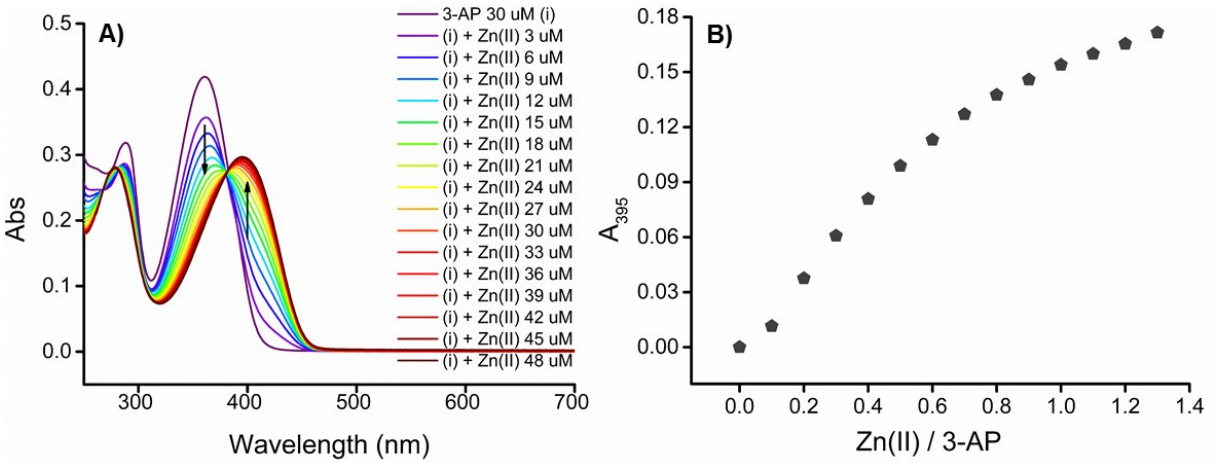

Fig. S17 Zn(II) titration of the ligand 3-AP.

A) UV-Vis spectra; B) corresponding binding curve at λ_{max} = 395 nm.

Experimental conditions: A 30 μM solution of 3-AP in 100 mM HEPES buffer pH 7.4, was titrated with 1 μL aliquots of a 300 μM Zn(II) stock solution.

Zn(II) addition to the 3-AP solution induced the appearance of two new bands in the UV-Vis region, respectively at λ_{max} = 395 nm and λ_{max} = 278 nm, along with the disappearance of the free ligand bands at 360 nm and 288 nm. (isosbestic point, λ = 380 nm).

Zn(II)-3-AP: λ_{max} = 395 nm, λ_{max} = 278 nm

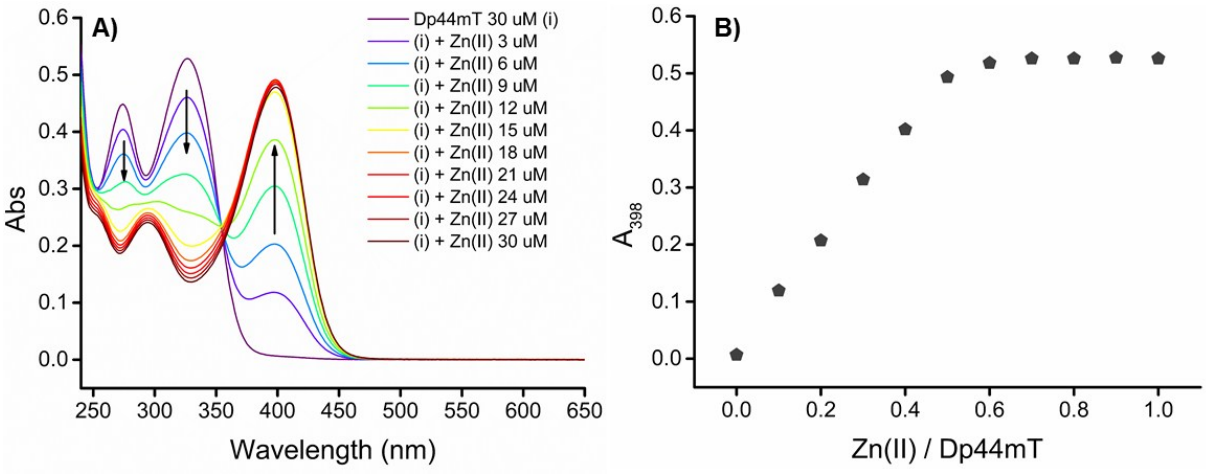

Fig. S18 Zn(II) titration of the ligand Dp44mT.

A) UV-Vis spectra; B) corresponding binding curve at λ_{max} = 398 nm.

Experimental conditions: A 30 μM solution of Dp44mT in HEPES buffer 100 mM, pH 7.4, was titrated with 1 μL aliquots of a 300 uM Zn(II) stock solution.

The formation of a complex Zn(II)-Dp44mT$_2$ with a distinct 1:2 stoichiometry was detected upon Zn(II) addition to the Dp44mT solution, shown by the increase in intensity of a new peak at λ_{max} = 398 nm, along with the appearance of a new band at λ_{max} = 294 nm, until 0.5 eq of Zn(II) with respect to Dp44mT. Simultaneously, in the UV-region, the bands of free Dp44mT at 326 nm and 274 nm disappeared. (isosbestic point, λ = 354 nm).

Zn(II)-Dp44mT$_2$: λ_{max} = 398 nm, λ_{max} = 294 nm

Reactivity of the Zn(II)-TSC complexes with GSH

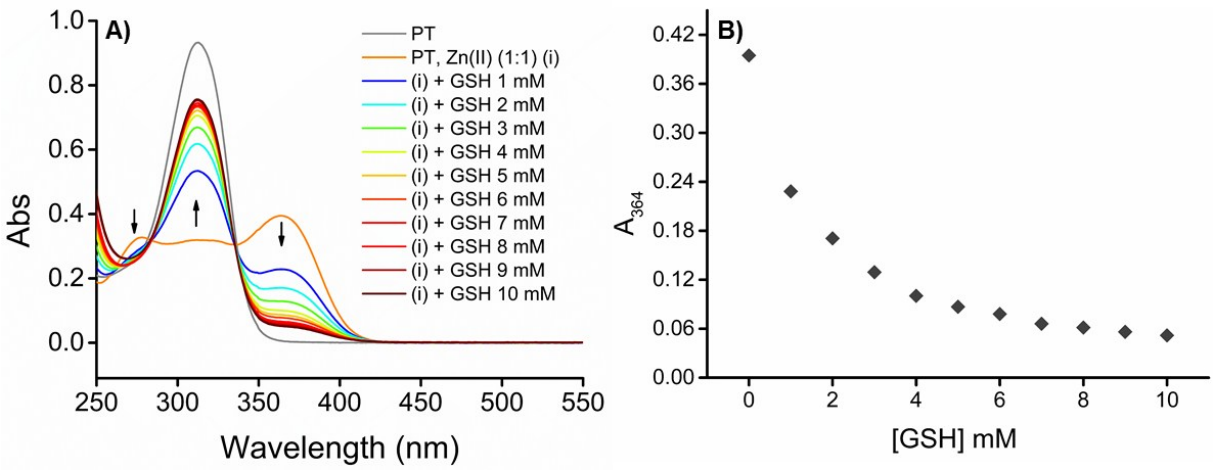

Fig. S19 Reactivity of Zn(II)-PT complex with GSH.

A) UV-Vis spectra; B) Absorbance at λ_{max} = 364 nm (CT band of the Zn(II)-PT complex) versus GSH concentration (mM).

Experimental conditions: to a 30 μM solution of PT and 30 μM of Zn(II) in HEPES buffer 100 mM, pH 7.4, 1 μL aliquots of a 100 mM stock solution of GSH were added to obtain the desired GSH concentration (from 1 to 10 mM).

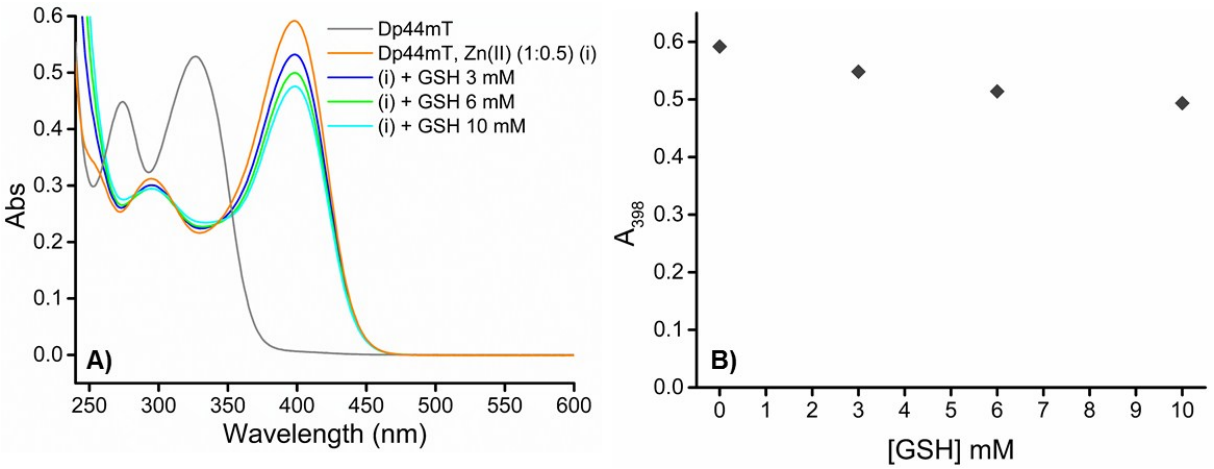

Fig S20 Reactivity of Zn(II)-Dp44mT$_2$ complex with GSH.

A) UV-Vis spectra; B) absorbance at λ_{max} = 398 nm (CT band of the Zn(II)-Dp44mT$_2$ complex) versus GSH concentration (mM).

Experimental conditions: To a 30 μM solution of Dp44mT and 15 μM of Zn(II) in HEPES buffer 100 mM, pH 7.4, 3, 6 and 10 μL of a 100 mM stock solution of GSH were added to obtain a final GSH concentration of 3, 6, 10 mM.

Reactivity of the Iron(II)-TSC complexes with Zn_7MT-1 and GSH

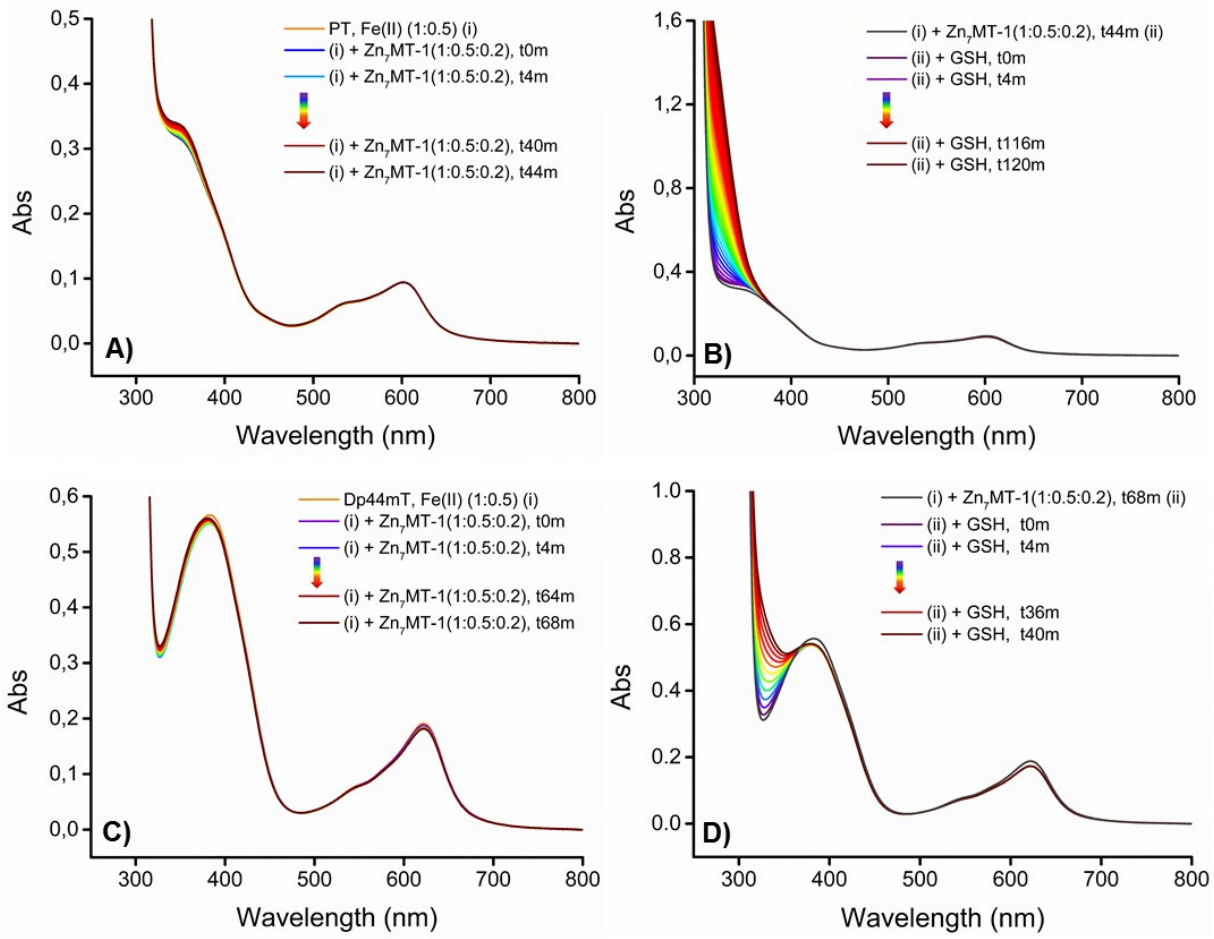

Fig. S21 Reactivity of Fe(II)-PT_2 and Fe(II)-Dp44mT_2 complexes with Zn_7MT-1 and GSH.

A) UV-Vis spectra for the reaction between Fe(II)-PT_2 and Zn_7MT-1; B) UV-Vis spectra for the reaction A after the addition of 3 mM GSH. C) UV-Vis spectra for the reaction between Fe(II)-Dp44mT_2 and Zn_7MT-1; D) UV-Vis spectra for the reaction C after the addition of 3 mM GSH.

Experimental conditions: The Fe(II)-PT_2 and Fe(II)-Dp44mT_2 complexes were generated by mixing a 30 uM solution of PT/Dp44mT with a 15 μM solution of Fe(III) in the presence of $AscH^-$ 5 mM (ratio (PT/Dp44mT:Fe(II), 1:0.5) in HEPES buffer 100 mM, pH 7.4 (λ_{max} Fe(II)-PT_2 = 600 nm, λ_{max} Fe(II)-Dp44mT_2 = 622 nm). To the preformed Fe(II)-PT/Dp44mT_2 complexes, 1.2 μL of a stock solution 494 μM of Zn_7MT-1 were added to obtain a final concentration of 6 μM. The reactions were monitored over time from t_0 min after Zn_7MT-1 addition to t_{44} min (Fe(II)-PT_2) and t_{68} min (Fe(II)-Dp44mT_2) , collecting each intermediate spectrum at 4 min intervals. To the mixture Fe(II)-PT/Dp44mT_2/Zn_7MT-1, 3 μL of a 100 mM stock solution of GSH were added to obtain a final GSH concentration of 3 mM, and the reactions were monitored over time for 120 min and 40 min, respectively.